Mixed-mode oscillations via canard explosions in light-emitting diodes with optoelectronic feedback

F. Marino,[1] M. Ciszak,[2] S. F. Abdalah,[2,3] K. Al-Naimee,[2,4] R. Meucci,[2] and F. T. Arecchi[1,2]
[1]*Dipartimento di Fisica, Università di Firenze, Via Sansone 1, I-50019 Sesto Fiorentino, Firenze, Italy*
[2]*Consiglio Nazionale delle Ricerche, Istituto Nazionale di Ottica, Largo E. Fermi 6, I-50125 Firenze, Italy*
[3]*High Institute of Telecommunications and Post, Al Salihiya, Baghdad, Iraq*
[4]*Department of Physics, College of Science,University of Baghdad, Al Jadiriah, Baghdad, Iraq*
(Received 18 February 2011; revised manuscript received 19 September 2011; published 24 October 2011)

Chaotically spiking attractors in semiconductor lasers with optoelectronic feedback have been recently observed to be the result of canard phenomena in three-dimensional phase space (incomplete homoclinic scenarios). Since light-emitting diodes display the same dynamics and are much more easily controllable, we use one of these systems to complete the attractor analysis demonstrating experimentally and theoretically the occurrence of complex sequences of periodic mixed-mode oscillations. In particular, we investigate the transition between periodic and chaotic mixed-mode states and analyze the effects of the unavoidable experimental noise on these transitions.

DOI: 10.1103/PhysRevE.84.047201 PACS number(s): 05.45.−a, 42.65.Sf

Oscillatory dynamics in chemical, biological, and physical systems often takes the form of complex temporal sequences known as mixed-mode oscillations (MMOs) [1]. Typical time traces are characterized by a mixture of L large-amplitude relaxation spikes followed by S small-amplitude quasiharmonic oscillations, while oscillations of intermediate amplitude do not occur. Sequences of this type are ubiquitous in nature and were originally observed in chemical systems more than 100 years ago [2], with the Belouzov-Zhabotinsky reaction being the most thoroughly studied example [3–6]. More recent studies involved surface chemical reactions [7–9], electrochemical systems [10,11], neural and cardiac cells [12,13], calcium dynamics [14], and plasma physics [15], to name just a few. As some bifurcation parameter is varied, MMOs can be ordered in periodic-chaotic sequences, in which intervals of periodic states are separated by chaotic states resembling random mixtures of the adjacent periodic patterns. In other cases, these mixtures can form periodic concatenations following the Farey arithmetic and plotting of a suitably defined winding number against the bifurcation parameter leads to a devil's staircase.

Several mechanisms can be at the origin of these phenomena [1], for instance, the quasiperiodic route to chaos on an invariant 2-torus [16] and the loss of stability of a Shilnikov homoclinic orbit [17,18]. However, periodic-chaotic sequences and Farey sequences of MMOs do not necessarily involve a torus or a homoclinic orbit, but can occur also through the canard phenomenon [19]. Here a limit cycle born in a supercritical Hopf bifurcation experiences the abrupt transition from a small-amplitude quasiharmonic cycle to large relaxation oscillations in a narrow parameter range (canard explosions) [20]. Although this sudden transition can be easily misinterpreted as a homoclinic bifurcation, here an exact homoclinic connection to a saddle focus does not occur and therefore application of the Shilnikov theorem is not allowed. Such behavior is typical in three-dimensional (3D) multiple-time-scale dynamical systems, which can be described in terms of a fast 2D oscillatory subsystem, coupled to a slowly evolving variable acting as a quasistatic bifurcation parameter. The strong separation of time scales may induce the switch between periods of small amplitude and relaxation oscillations and makes the flow to pass very closely to the saddle-focus stationary state, thus simulating trajectories close to the Shilnikov condition. For this reason, canard phenomena in 3D systems are often referred to as incomplete homoclinic scenarios [21]. Although most of the studies of this dynamics have been carried out in chemical systems, incomplete homoclinic scenarios have been recently predicted and observed also in semiconductor lasers with optoelectronic feedback [22,23] and optical cavities with movable mirrors [24,25]. In these works, attention has been focused on the chaotically spiking regime, a special kind of MMO where large pulses are separated by an irregular number of quasiharmonic oscillations. In this Brief Report we complete the dynamical picture by extending the analysis also to regular types of MMOs. In particular, we investigate experimentally the transition between periodic and chaotic mixed-mode states and analyze the effects of the unavoidable experimental noise on these transitions.

The system here considered is a GaAs light-emitting diode (LED) (with a peak wavelength of 870 nm and spectral width of ∼50 nm) with ac-coupled nonlinear optoelectronic feedback. The LED is driven by a constant positive voltage via a current-limiting resistor (3 kΩ) in series. The output light is sent to a photodetector producing a signal directly proportional to the optical intensity in the whole operation range. The corresponding voltage signal is high-pass filtered (with a cutoff frequency of $\gamma_f \sim 1$ kHz) and amplified by means of a variable-gain amplifier characterized by a nonlinear transfer function of the form $f_F(w) = Aw/(1 + s'w)$, where A is the amplifier gain and s' is a saturation coefficient. The feedback voltage signal is then added to the dc voltage driving the LED by means of a mixer.

As will be clarified later, a key element to observe MMOs in optoelectronic devices is the existence of a threshold for light emission. In semiconductor lasers this is the current value at which gain (stimulated emission) overcomes the cavity losses. In LEDs the main recombination mechanism is spontaneous emission and the emitted light is simply proportional to the current passing through the device. However, as in electronic diodes, the current-voltage characteristics of a LED are highly nonlinear. With no external applied voltage, an equilibrium

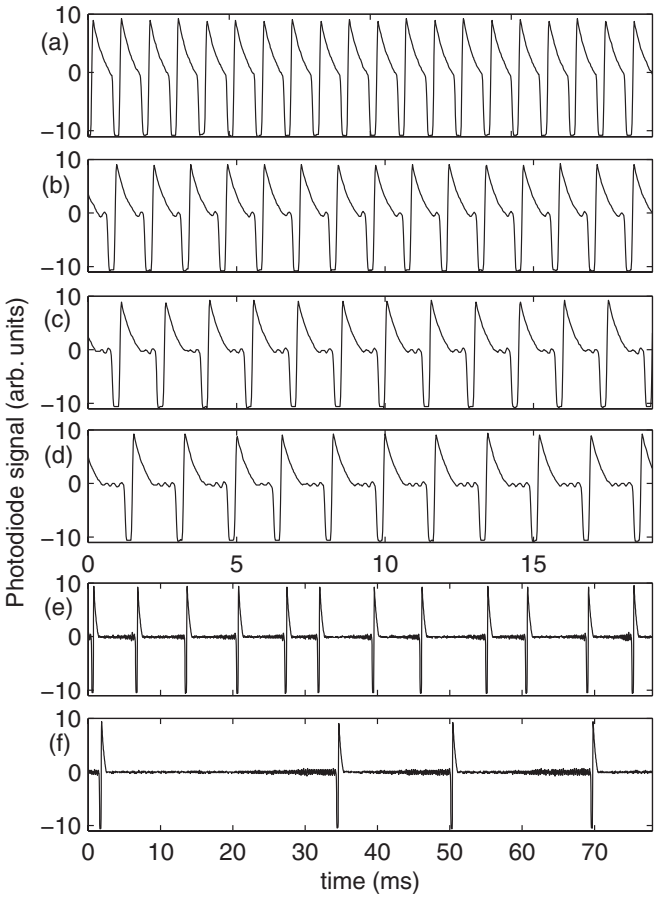

FIG. 1. Experimental time series of the optical intensity as V_n is decreased: (a) $V_n = 0.0558$, (b) $V_n = 0.0392$, (c) $V_n = 0.0242$, (d) $V_n = 0.0163$, (e) $V_n = 0.0046$, and (f) $V_n = 0.0027$.

condition is reached in which a built-in potential $V_{\rm bi}$ prevents electron and hole diffusion across the p-n junction. A current flow as well as the consequent emission of light via electron-hole recombination is established only if a forward voltage $V_d > V_{\rm bi}$ is applied to the junction. As a consequence, the light-voltage curve shows a threshold voltage approximately equal to $V_{\rm bi}$.

In order to characterize the system dynamics, we define the dimensionless control parameter $V_n = (V_0 - V_{\rm th})/V_{\rm th}$, where V_0 is the externally applied voltage, and assign the symbolic notation L^S to the MMO states, where L gives the number of large-amplitude oscillations and S the number of small-amplitude oscillations in a single periodic pattern. The relaxation oscillation regime 1^0 [see Fig. 1(a)] is the dominant behavior of the system, occurring in a very wide voltage range above threshold. The typical sequence of MMO states that is observed as V_n is decreased is shown in Figs. 1(b), 1(c), and 1(d), displaying 1^1-, 1^2-, and 1^3-periodic states, respectively. At lower values of V_n, a chaotically spiking regime sets in, where large-amplitude oscillations are separated by an irregular number of small-amplitude oscillations [see Fig. 1(e)]. Decreasing V_n even further, the mean interspike interval increases [Fig. 1(f)] until large-amplitude spikes disappear and the system eventually reaches a stationary state. The transition between such a stable state and the chaotically spiking regime, occurring through a cascade

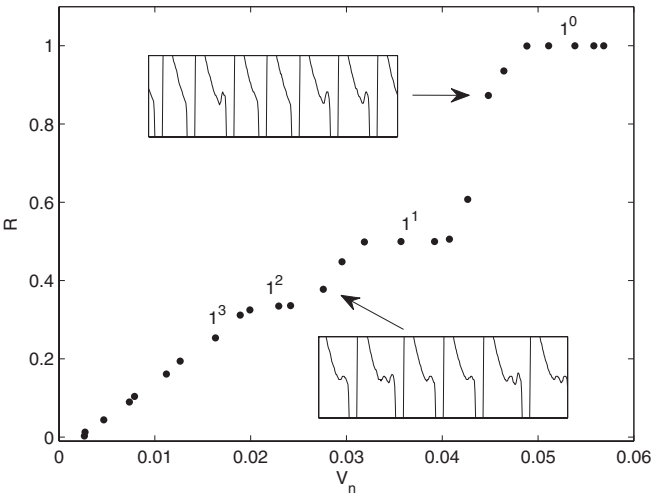

FIG. 2. Plot of the winding number R as a function V_n. Insets: Experimental time series of the optical intensity corresponding to $V_n = 0.0448$ and 0.0275.

of period-doubled and chaotic (small-amplitude) attractors, has been investigated in detail in Refs. [22,24]. Here we mainly focus on transitions between different periodic MMO states. The complete bifurcation diagram corresponding to the mixed-mode wave forms can be represented by plotting the winding number $R = L/(L + \langle S \rangle)$ as a function of the control parameter (see Fig. 2). In our system we have always $L = 1$ and hence states 1^0, 1^1, 1^2, and 1^3 have R equal to 1, 1/2, 1/3, and 1/4, respectively. In the transition between these states, random concatenations of the adjacent patterns are observed. The insets in Fig. 2 show two examples of these concatenations between 1^0 and 1^1 states and between 1^1 and 1^2 states. Here R is calculated from the mean value of S over all the periodic intervals in the time series. As a result, in a transition between 1^S and 1^{S+1}, R changes between the values $1/(1 + S)$ and $1/(1 + S + 1)$, depending on the number of 1^S or 1^{S+1} patterns observed in the time series. Although similar to the periodic-chaotic sequences often observed between periodic MMO states, the model that we introduce later does not show such concatenations. This suggests that this behavior could be due to the effect of noise, which sporadically drives the system over the transitions. Therefore, we cannot resolve the details of the devil's staircase that should accompany the transition between periodic mixed-mode states. In the chaotically spiking regime ($V_n \lesssim 0.013$) R is observed to continuously decrease to zero with the increasing mean interspike interval and the subsequent disappearance of large-amplitude spikes.

The simplest approach is to phenomenologically model the LED as an ideal p-n junction with a uniform recombination region of cross-sectional area S and width Δ. The system dynamics is then determined by three coupled variables, the carrier (electron) density N, the junction applied voltage V_d, and the high-pass-filtered feedback voltage V_f, evolving with very different characteristic time scales

$$\dot{N} = -\gamma_{\rm sp} N + \frac{\mu N (V_d - V_{\rm bi})}{\Delta^2}, \tag{1}$$

$$C\dot{V}_d = \frac{V_0 - V_d + f_F(V_f)}{R} - \frac{e\mu N S (V_d - V_{\rm bi})}{\Delta}, \tag{2}$$

$$\dot{V}_f = -\gamma_f V_f + k\dot{\Phi}, \tag{3}$$

where γ_{sp} is the spontaneous emission rate, μ is the carrier mobility, C is the diode capacitance (here assumed to be voltage independent for simplicity), V_0 is the dc bias voltage, R is the current-limiting resistor, $f_F(V_f)$ is the feedback amplifier function, e is the electron charge, k is the photodetector responsivity, and Φ is the photon density, which is assumed to be linearly proportional to the carrier density $\Phi = \eta N$, where η is the LED quantum efficiency. Equation (1) indicates that N in the active layer decreases due to radiative recombination and increases with the forward injection current density $J = e\mu N(V_d - V_{bi})/\Delta$. Nonradiative recombination and carrier generation by optical absorption have been neglected since we checked that they do not significantly change the dynamics. Equation (2) is the Kirchhoff law of the circuit (resistor-ideal diode) relating the junction voltage V_d to the dc applied voltage V_0 [the second term in Eq. (2) is the current flow across the diode $I = JS$]. Equation (3) describes the nonlinear feedback loop where the voltage signal coming from the detector $k\Phi$ is high-pass filtered and added to the dc bias through the amplifier function $f_F(V_f)$. Consider just the solitary LED equations (1) and (2). A finite stationary carrier density, increasing linearly with V_0, is found only when $V_d > V_{th} \equiv V_{bi} + \frac{\gamma_{sp}\Delta^2}{\mu}$; otherwise, the only stationary solution is $N = 0$ and $V_d = V_0$ (zero current). Accordingly, light emission begins when the applied voltage V_0 exceeds the threshold voltage V_{th}. By introducing the dimensionless variables $x = \frac{e\mu RSN}{\Delta}$, $y = \frac{\mu(V_d - V_{bi})}{\Delta\gamma_{sp}}$, and $w = \frac{e\mu RS}{k\eta\Delta}V_f - x$ and the time scale $t' = \gamma_{sp}t$ Eqs. (1)–(3) become

$$\dot{x} = x(y-1), \tag{4}$$

$$\dot{y} = \gamma[\delta_0 - y + f(w+x) - xy], \tag{5}$$

$$\dot{w} = -\varepsilon(w+x), \tag{6}$$

where $f(w+x) \equiv \alpha\frac{w+x}{1+s(w+x)}$, $\delta_0 = (V_0 - V_{bi})/(V_{th} - V_{bi})$, $\gamma = 1/RC\gamma_{sp}$, $\varepsilon = \gamma_f/\gamma_{sp}$, $\alpha = Ak\eta/e\gamma_{sp}R\Delta S$, and $s = k\eta\Delta s'/e\mu RS$.

Notice that the model Eqs. (4)–(6) is identical to that describing a single-mode laser diode in the presence of the same optoelectronic feedback loop [22]. In this case, x and y are suitably normalized photon and population-inversion densities and γ is the ratio between photon and carrier lifetimes. The dynamical mechanism underlying MMOs in such a system has been analyzed in detail in Ref. [22]. Here we just summarize its main features, discussing the similarities between laser and LEDs dynamics. In correspondence with the laser threshold $\delta_0 = 1$, the system undergoes a transcritical bifurcation where the zero-intensity solution and the lasing solution become unstable and stable, respectively. The introduction of a third degree of freedom (and a third, much slower time scale) describing the nonlinear ac feedback loop has two main effects: (i) Above threshold the stationary lasing solution loses stability through a supercritical Hopf bifurcation and is then followed by a cascade of period-doubled and chaotic attractors of small amplitude and (ii) the system becomes a singularly perturbed system of three time scales with a one-dimensional S-shaped slow manifold. On this manifold, the lower attractive branch is a straight line given by the zero-intensity solution $\{x = 0, y_w = \delta_0 + f(w), w\}$, while the middle repulsive and upper attractive branches are determined by the feedback nonlinear transfer function [22]. Since two branches rapidly attract all neighboring trajectories while the middle branch repels them, canard and relaxation cycles arise. However, in 3D phase space, there is also room for more complex scenarios, where relaxation orbits are separated by a certain number of small-amplitude oscillations surrounding the steady state of the system P. When lying on the middle repelling branch, this point is a saddle focus and a trajectory rotates around P before switching to the other stable branch of the manifold. The number of these rotations, as well as the periodic or erratic nature of MMOs, is determined by the rates at which y and w vary in the vicinity of P. This is not simply related to γ and ε, but also depends on the bifurcation parameter δ_0. Therefore, apart the feedback loop, the key element to observe this dynamics is a 2D solitary system possessing a threshold and governed by two different characteristic time scales. In this framework, LEDs are dynamically equivalent to semiconductor lasers.

Figure 3 shows some of MMO patterns, obtained by numerical integration of Eqs. (4)–(6). As the parameter δ_0 is decreased, we observe the complete sequence of transitions going from the 1^0 state to the chaotically spiking regime, thus

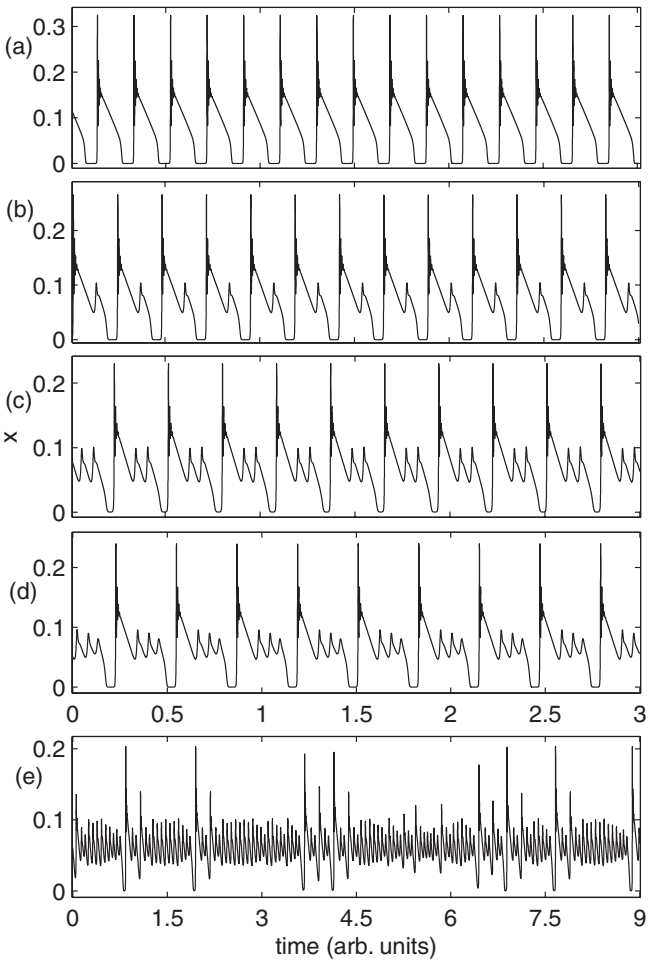

FIG. 3. Time series of the variable x as obtained by numerical integration of Eqs. (4)–(6): (a) $\delta_0 = 1.08$, (b) $\delta_0 = 1.07$, (c) $\delta_0 = 1.067$, (d) $\delta_0 = 1.065$, and (e) $\delta_0 = 1.06$. The fixed parameters are $\alpha = 1.002$, $\gamma = 3.3 \times 10^{-3}$, $\varepsilon = 4 \times 10^{-5}$, and $s = 0.2$.

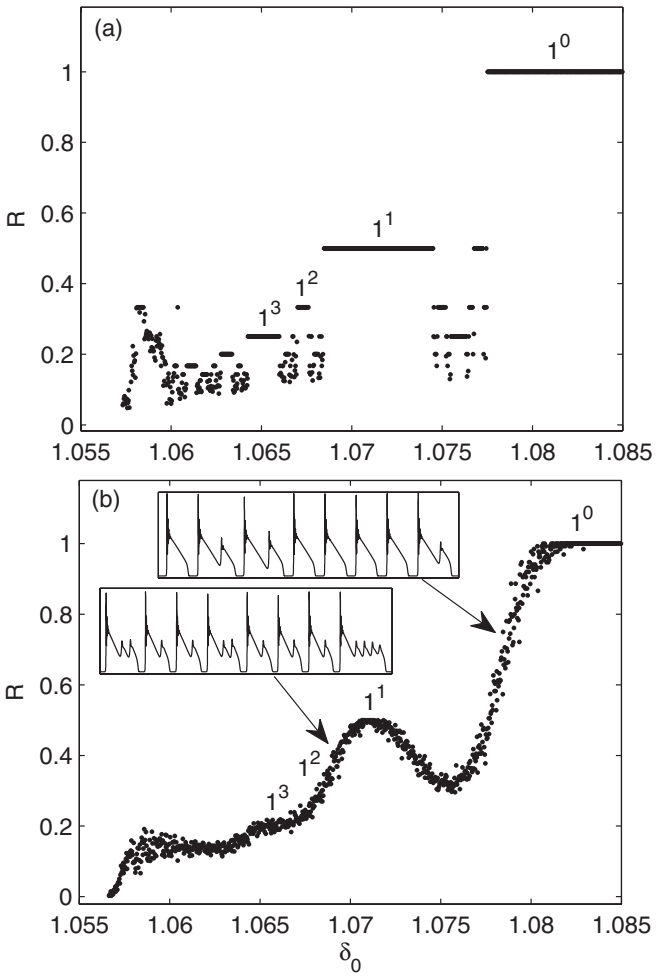

FIG. 4. (a) Plot of the winding number R as a function of δ_0 for the model equations (4)–(6). (b) Same as in (a), but under the white-noise effect of amplitude $D = 3 \times 10^{-5}$. Insets: Time series of the variable x corresponding to $\delta_0 = 1.075$ and 1.069. Other parameters are the same as in Fig. 3.

reproducing qualitatively the experimental results. However, in contrast to the experiment, the detailed bifurcation diagram in terms of the winding number R reveals an extraordinary complexity [see Fig. 4(a)]. Between the main 1^S-$1^{(S+1)}$ transitions, the system displays a (presumably infinite) number of periodic mixed-mode windows and, in some cases between them, chaotically spiking time series. A detailed study of Eqs. (4)–(6) showing the complex organization of MMOs domains in the parameter space has been recently reported in Ref. [26]. In our experiment, however, these narrow intermediate windows have not been observed. In their place, the system exhibits random concatenations of adjacent states 1^S-1^{S+1} (see Fig. 2), unobserved in numerical simulations. These differences can be explained considering the presence of experimental noise, whose effects are particularly important in the vicinity of bifurcations. Assuming the driving voltage noise as the dominant noise source in the system, we performed numerical simulations by adding a small stochastic term to the voltage equation (5). The corresponding plot of R as a function of δ_0, reported in Fig. 4(b), confirms that one of the noise effects is to sporadically drive the system over adjacent transitions. This is evidenced by the time series in the insets in Fig. 4(b), where random concatenations of parent states similar to those observed in the experiment are displayed. A further effect of noise is to hide the narrow intermediate windows between the main periodic states. However, their existence is revealed by the presence of some errors, as shown, for instance, in the upper inset in which a 1^4 event in a 1^1-1^2 concatenation is observed. Since in the experiment such errors have not been reported, we conclude that probably these narrow periodic windows are simply less pronounced than in the model.

In conclusion, we reported experimental evidence of complex periodic mixed-mode oscillations in a light-emitting diode with optoelectronic feedback. The complete transition diagram between periodic and chaotic mixed-mode states has been characterized and the role of experimental noise on these transitions has been investigated. The experimental results have been qualitatively reproduced by a simple physical model of the system.

M.C. acknowledges MC-ERG (7th EC Programme) and S.F.A. acknowledges ICTP-TRIL for financial support. This work was partly supported by the contract "Dinamiche Cerebrali Caotiche" of Ente Cassa di Risparmio di Firenze.

[1] For a review, M. Brons, T. Kaper, and H. G. Rotstein, eds., see Chaos **18**(1) (2008), special issue on mixed-mode oscillations: experiment, computation, and analysis.
[2] W. Ostwald, Z. Phys. Chem. Stoechiom. Verwandtschaftsl. **35**, 33 (1900).
[3] R. A. Schmitz, K. R. Graziani, and J. L. Hudson, J. Chem. Phys. **67**, 3040 (1977).
[4] K. Showalter, R. M. Noyes, and K. Bar-Eli, J. Chem. Phys. **69**, 2514 (1978).
[5] J. Maselko and H. L. Swinney, Phys. Lett. A **119**, 403 (1987).
[6] M. Brøns and K. Bar-Eli, J. Phys. Chem. **95**, 8706 (1991).
[7] M. Bertram and A. S. Mikhailov, Phys. Rev. E **63**, 066102 (2001).
[8] M. Bertram *et al.*, Phys. Rev. E **67**, 036208 (2003).
[9] M. Kim *et al.*, Science **292**, 1357 (2001).
[10] M. T. M. Koper, Physica D **80**, 72 (1995).
[11] F. Plenge, P. Rodin, E. Scholl, and K. Krischer, Phys. Rev. E **64**, 056229 (2001).
[12] A. A. Alonso and R. R. Llinás, Nature (London) **342**, 175 (1989).
[13] G. S. Medvedev and J. E. Cisternas, Physica D **194**, 333 (2004).
[14] U. Kummer *et al.*, Biophys. J. **79**, 1188 (2000).
[15] M. Mikikian, M. Cavarroc, L. Couedel, Y. Tessier, and L. Boufendi, Phys. Rev. Lett. **100**, 225005 (2008).
[16] R. Larter and C. G. Steinmetz, Philos. Trans. R. Soc. London Ser. A **337**, 291 (1991).
[17] A. Arneado, F. Argoul, J. Elezgaray, and P. Richetti, Physica D **72**, 134 (1993).
[18] M. T. M. Koper, Physica D **80**, 72 (1995).

[19] M. Brøns, M. Krupa, and M. Wechselberger, Fields Inst. Comm. **49**, 39 (2006); M. Krupa, N. Popovic, and N. Kopell, SIAM J. Appl. Dyn. Syst. **7**, 361 (2008); J. Guckenheimer, *ibid.* **7**, 1355 (2008); J. Guckenheimer and C. Scheper, *ibid.* **10**, 92 (2011).
[20] E. Benoit, J. L. Callot, F. Diener, and M. Diener, Collect. Math. **32**, 37 (1981).
[21] M. T. M. Koper, P. Gaspard, and J. H. Sluyters, J. Chem. Phys. **97**, 11 (1992).
[22] K. Al-Naimee, F. Marino, M. Ciszak, R. Meucci, and F. T. Arecchi, New J. Phys. **11**, 073022 (2009).
[23] K. Al-Naimee *et al*., Eur. Phys. J. D **58**, 187 (2010).
[24] F. Marino, F. Marin, S. Balle, and O. Piro, Phys. Rev. Lett. **98**, 074104 (2007).
[25] F. Marino and F. Marin, Phys. Rev. E **83**, 015202 (2011).
[26] J. G. Freire and J. A. C. Gallas, Phys. Rev. E **82**, 037202 (2010).